



# Anodizing Properties of High Dielectric Oxide Films Coated on Aluminum by Sol-Gel Method

SANG-SHIK PARK<sup>1,\*</sup> & BYONG-TAEK LEE<sup>2</sup>

<sup>1</sup>Department of Materials Science and Engineering, Sangju National University, 386, Gajang-dong, Sangju, Kyungbuk 742-711, Korea

<sup>2</sup>School of Advanced Materials Engineering, Kongju National University, 182, Sinkwan-dong, Kongju, Chungnam 314-701, Korea

Submitted February 12, 2003; Revised March 8, 2004; Accepted April 26, 2004

**Abstract.** In order to obtain the high capacitance in aluminum electrolytic capacitor, ZrO<sub>2</sub> and Nb<sub>2</sub>O<sub>5</sub> films were coated on aluminum foils by sol-gel method, and then the properties of anodized films were examined. The triple layer of ZrO<sub>2</sub>/Al-Zr(Nb)O<sub>x</sub>/Al<sub>2</sub>O<sub>3</sub> was formed on aluminum substrates after anodizing of ZrO<sub>2</sub>(Nb<sub>2</sub>O<sub>5</sub>)/Al film. The thickness of Al<sub>2</sub>O<sub>3</sub> layer decreased with increasing the annealing temperature due to the densification of ZrO<sub>2</sub> film and the capacitance of ZrO<sub>2</sub> coated aluminum foil annealed at low temperature was higher than that at high temperature. The increase of capacitance was due to the high capacitance of ZrO<sub>2</sub> film annealed at low temperature. The capacitance of ZrO<sub>2</sub> and Nb<sub>2</sub>O<sub>5</sub> coated aluminum increased about 3 and 1.7 times compared to that of Al<sub>2</sub>O<sub>3</sub> layer anodized with 400 V, respectively. From these results, the aluminum foils with composite oxide layers are found to be applicable to the aluminum electrolytic capacitor.

**Keywords:** Al electrolytic capacitor, sol-gel, anodizing, ZrO<sub>2</sub>, Nb<sub>2</sub>O<sub>5</sub>

## 1. Introduction

Aluminum electrolytic capacitors, which are passive electronic parts, have been widely used in electric and electronic devices. Anodized aluminum oxide, Al<sub>2</sub>O<sub>3</sub> has been used as dielectric material of aluminum electrolytic capacitor and the capacitance of the electrolytic capacitor is expressed by the following equation.

$$C = (\epsilon_0 \cdot \epsilon_r \cdot A) / d$$

where,  $C$  is capacitance,  $\epsilon_0$  permittivity in vacuum,  $\epsilon_r$  dielectric constant of oxide film,  $A$  the surface area of electrode, and  $d$  thickness of dielectrics. Increase of capacitance in the capacitor of same volume can be obtained by increase of  $\epsilon_r$  and  $A$  and decrease of  $d$ , whereas in order to increase the withstanding voltage, the thickness of dielectrics must be increased. Recent trends for small electronic devices require high capacitance of electrolytic capacitors, and so extensive stud-

ies have been performed to increase the capacitance. Many researches were focused on an enlargement of surface area and improvement of oxide properties [1–3]. Though the surface area was enlarged greatly by electrochemical etching method, the development of smaller capacitor was very difficult because an enlargement of the surface area by etching process was faced with the limit. Increase in dielectric constant of oxide films is very important in addition to increase of surface area and decrease in film thickness, therefore the application of high dielectric material is necessary for the increase of capacitance. Increase in dielectric constant may be possible by incorporating valve metal oxides as such Ta<sub>2</sub>O<sub>5</sub>, Nb<sub>2</sub>O<sub>5</sub>, TiO<sub>2</sub>, ZrO<sub>2</sub> and others. In this study, aluminum foils were coated with ZrO<sub>2</sub> and Nb<sub>2</sub>O<sub>5</sub> films by sol-gel method. Up to now, the properties of ZrO<sub>2</sub> and Nb<sub>2</sub>O<sub>5</sub> films for various applications were shown by PVD (physical vapor deposition) and chemical method, but many problems were involved in capacitor application. Takahashi et al. demonstrated the properties of aluminum composite oxide films prepared by pore-filling method [4], MOCVD (Metal-organic Chemical Vapor Deposition) [5] and sol-gel method

\*To whom all correspondence should be addressed. E-mail: sspark@sangju.ac.kr

[6] for aluminum electrolytic capacitor. In this work,  $ZrO_2$  and  $Nb_2O_5$  films were coated by sol-gel method and films were annealed at various temperature. The crystal structure, interface and dielectric properties of films were studied with annealing temperature after anodizing.

## 2. Experimental

The  $ZrO_2$  films were obtained from the solution containing zirconium *n*-butoxide [ $Zr[O(CH_2)_3CH_3]_4$  (Aldrich), 0.05 mol/l], 2 methoxy ethanol [ $CH_3OCH_2CH_2OH$ ], Diethanolamine [ $(HOCH_2CH_2)_2NH$ ] and de-ionized water (100:10:1.5) and  $Nb_2O_5$  films from niobium butoxide [ $Nb(OC_2H_5)_5$  (Aldrich), 0.05 mol/l], 2 methoxy ethanol, acetic acid and de-ionized water (100:0.02:1.0). High purity Al foil (99.99%, 100  $\mu m$ ) was used as substrate after electro-polishing in a perchloric acid and acetic acid mixture. The electro-polished substrates were coated by sol-gel dip method with the procedure indicated in Fig. 1. The coated films showed the thickness of 15–20 nm per cycle for  $ZrO_2$  films and 30–35 nm per cycle for  $Nb_2O_5$  films. The foils coated with  $ZrO_2$  and  $Nb_2O_5$  films were dried at 150°C and annealed at vacuum furnace for 60 min. The annealed specimens were anodized by capacitor charging power supply (Fug, HCK 750M-1250) with a constant current of 10 A/m<sup>2</sup> in water (1000 ml) and boric acid ( $H_3BO_3$ , 70 g) mixture of pH 3.2. The change in the anode potential with time during an-

odizing was monitored by a PC system. The micro-structure and thickness of specimens were determined using field emission scanning electron microscopy (FE-SEM (TOPCON DS-130C)) and transmission electron microscopy (TEM (JEM 2010)). The composition of films was identified by Rutherford backscattering spectroscopy (RBS (NEC 3SDH)) using 2.236 MeV  $4He^{2+}$  ion and energy dispersive X-ray spectroscopy (EDS). The capacitance and dissipation factor as a function of frequency were measured with impedance-gain phase analyzer (HP 4194A) after anodized two specimens were immersed in parallel at water (1000 ml) and ammonium adipate (150 g) mixture.

## 3. Results and Discussion

Figure 2 shows the TEM images of  $ZrO_2$  films anodized up to 200 V and  $Nb_2O_5$  films anodized up to 400 V after 6th coating. The  $ZrO_2$  layer annealed at 300°C of Fig. 2(a) shows a uniform thickness, and the anodized specimen shows two layers below  $ZrO_2$  layer. The two layers were identified as Al-Zr composite oxide and  $Al_2O_3$  layer by EDS and RBS analyses. It may be considered that the growth of aluminum oxide layer during anodizing is due to that  $O^{2-}$  ions dissociated from water or electrolyte at the bottom of the  $ZrO_2$  layer transport inwards across the anodic oxide film to form pure aluminum oxide at the interface between the Zr-oxide layer and Al substrate. The diffraction pattern of right upper end obtained from  $ZrO_2$  layer suggested that  $ZrO_2$  layer annealed at 300°C had crystalline structure. Figure 2(b) shows the HRTEM surface image of  $ZrO_2$  layer annealed at 300°C. As can be expected from diffraction pattern of Fig. 2(a), the lattice image of surface shows that  $ZrO_2$  layer is composed of polycrystal of nano-size. Figure 2(c) shows the cross-section image of  $ZrO_2$  layer annealed at 600°C. The specimen shows only a part of  $ZrO_2$  layer at surface due to exfoliation during the preparation of TEM sample, and this suggests that the  $ZrO_2$  layer annealed at 600°C shows poorer adhesion than that at 300°C. Judging from that many samples show the same results, it may be assumed that the bonding force of  $ZrO_2$  layer with substrate decrease by the stress of film due to the annealing at high temperature. Figure 2(d) shows TEM image of  $Nb_2O_5$  films anodized up to 400 V after 6th coating and annealing at 600°C.  $Nb_2O_5$  coated aluminum foil also showed two layers below crystalline  $Nb_2O_5$  layer and the layers consisted of Al-Nb composite oxide and

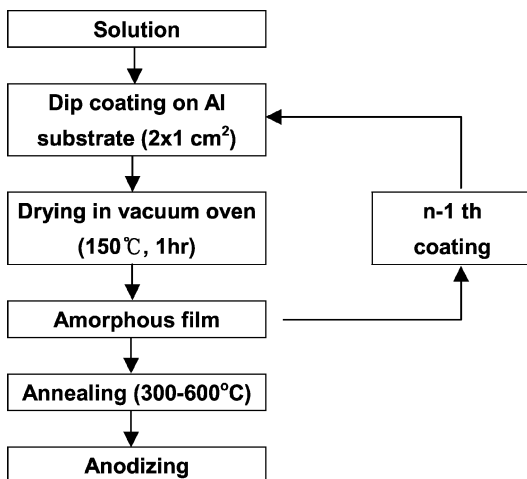


Fig. 1. Procedures for preparation of  $ZrO_2$  and  $Nb_2O_5$  films.

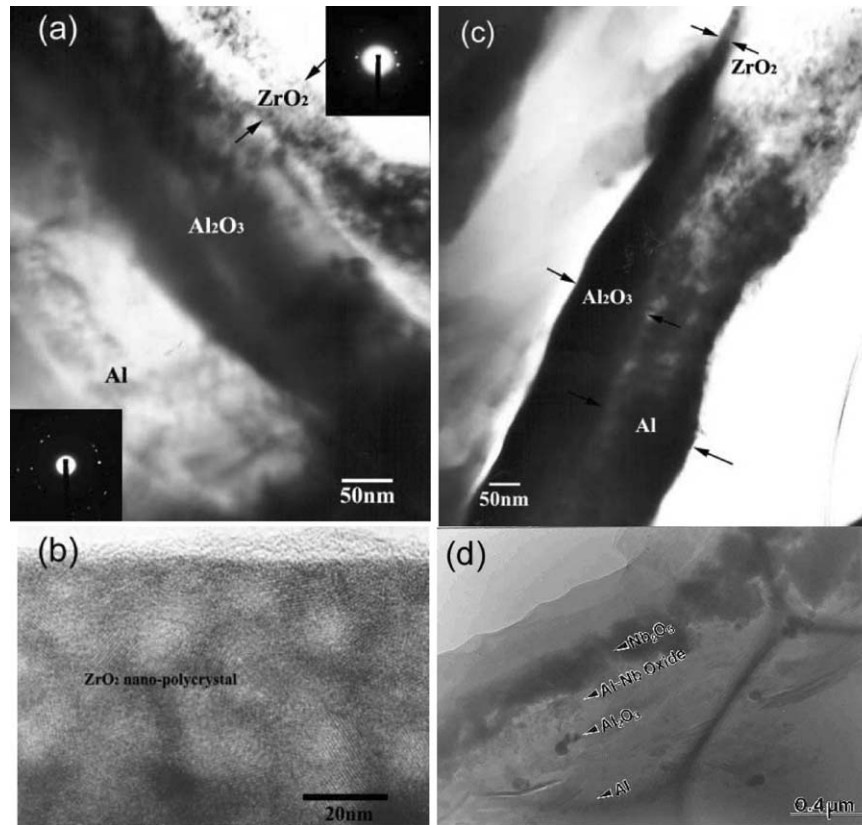


Fig. 2. TEM images of  $ZrO_2$  and  $Nb_2O_5$  films anodized with 200 and 400 V, respectively. Annealing temperature was  $300^\circ C$  in (a) and (b) and  $600^\circ C$  in (c) and (d).

$Al_2O_3$  layer. These results suggest that the composite oxide layers are formed irrelevant to coating materials after anodizing. When the  $ZrO_2$  coated and non-coated Al specimens were anodized up to 400 V with constant current of  $10 A/m^2$ ,  $Al_2O_3$  layer showed the thickness of 440 and 510 nm, respectively. The anodic oxide films composed of an amorphous oxide have the growth rate of 1.3–1.7 nm/V [7–9] and crystalline anodic oxide films after thermal treatment have 0.8–1.3 nm/V [10–12]. The  $Al_2O_3$  layer of  $ZrO_2$  coated specimens show thinner and denser structure compared to that of non-coated specimens. Considering these results, it may be assumed that dense crystalline  $ZrO_2$  layer in surface inhibited the inward diffusion of  $O^{2-}$  ions in electrolyte.

Figure 3 shows the RBS spectra and concentration depth profile obtained from  $ZrO_2$  and  $Nb_2O_5$  coated specimens. Figure 3(b) shows that oxide layer consists of  $ZrO_2/Al-ZrO_x/Al_2O_3$  on aluminum substrate and the thickness of  $ZrO_2$  and  $Al-ZrO_x$  layer is about 95 and

55 nm, respectively. Watanabe et al. reported [13] that Al-Zr composite oxide was not formed in films annealed at  $600^\circ C$  after repeat of coating and heat treatment at  $300^\circ C$ , however, in this study, Al-Zr composite oxide was formed after annealing at  $600^\circ C$ . This may be explained from that  $Al^{3+}$ ,  $Zr^{4+}$  and  $O^{2-}$  ions are diffused easily due to increase of micro-crack and pore because films are heat-treated at  $600^\circ C$  finally after repeat of coating and drying at  $150^\circ C$ . Figure 3(d) shows the concentration profiles of Nb, Al and O in depth, which is obtained by an analysis of Fig. 3(c). The triple layer of  $Nb_2O_5/Al-NbO_x/Al_2O_3$  was formed on aluminum substrate, which was similar to  $ZrO_2$  coating and the thickness of  $Nb_2O_5$  and  $Al-NbO_x$  layer was about 180 and 98 nm, respectively.

Figure 4(a) shows the change of the anode potential with anodizing time after  $ZrO_2$  coating of 6 times. The anode potential of specimen without annealing did not rise due to evaporation of organic compound. The

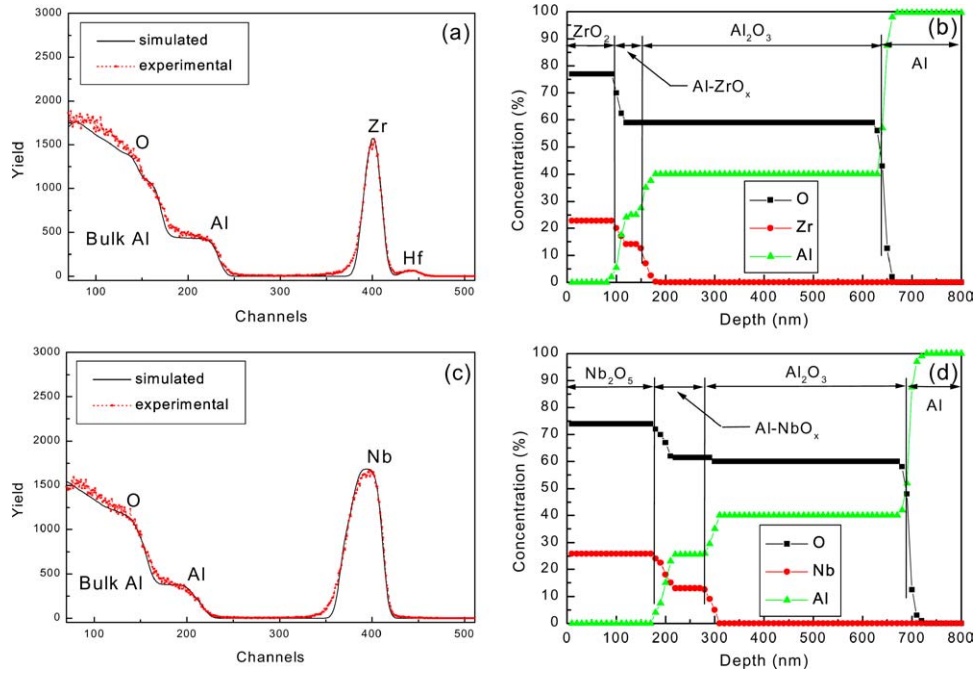


Fig. 3. RBS spectra and concentration depth profiles of ZrO<sub>2</sub> and Nb<sub>2</sub>O<sub>5</sub> films anodized with 400 V. ZrO<sub>2</sub> (a, b) and Nb<sub>2</sub>O<sub>5</sub> (c, d) films were coated 6 times and annealed at 600°C.

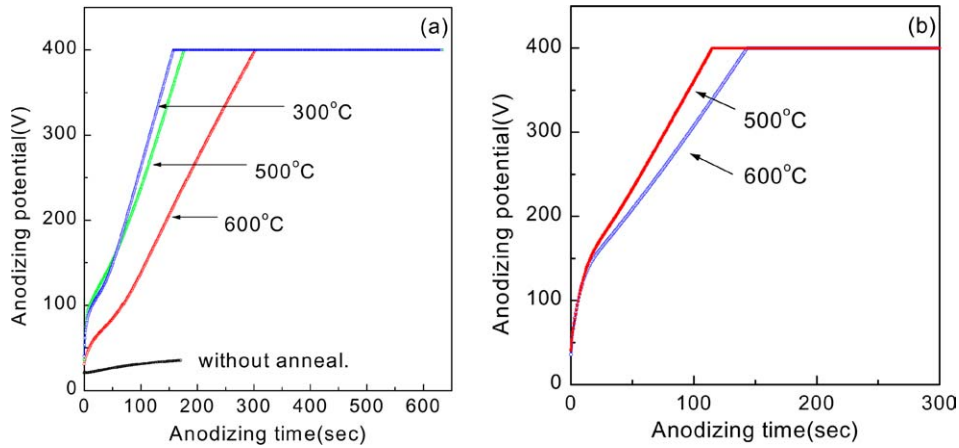


Fig. 4. Variations of anode potential with applying time for (a) ZrO<sub>2</sub> and (b) Nb<sub>2</sub>O<sub>5</sub> films annealed at various temperature.

annealed specimens show a linear increase in anode potential and the slope of potential curve become flatter with increasing annealing temperature. The result of Fig. 2, that the thickness of Al<sub>2</sub>O<sub>3</sub> in film annealed at 600°C is thinner than that at 300°C, can be explained by slow anodizing of films anodized at high temperature. This result suggests that the crystallinity and density

of ZrO<sub>2</sub> increase due to heating at 500 and 600°C, and then, inward diffusion of O<sup>2-</sup> ions from electrolyte is more difficult. Also, Nb<sub>2</sub>O<sub>5</sub> film of Fig. 4(b) shows the similar behavior to ZrO<sub>2</sub> film.

Aluminum foils without oxide coating were anodized for comparison to oxide coated aluminum foil. Figure 5 shows the capacitance and dissipation factor of

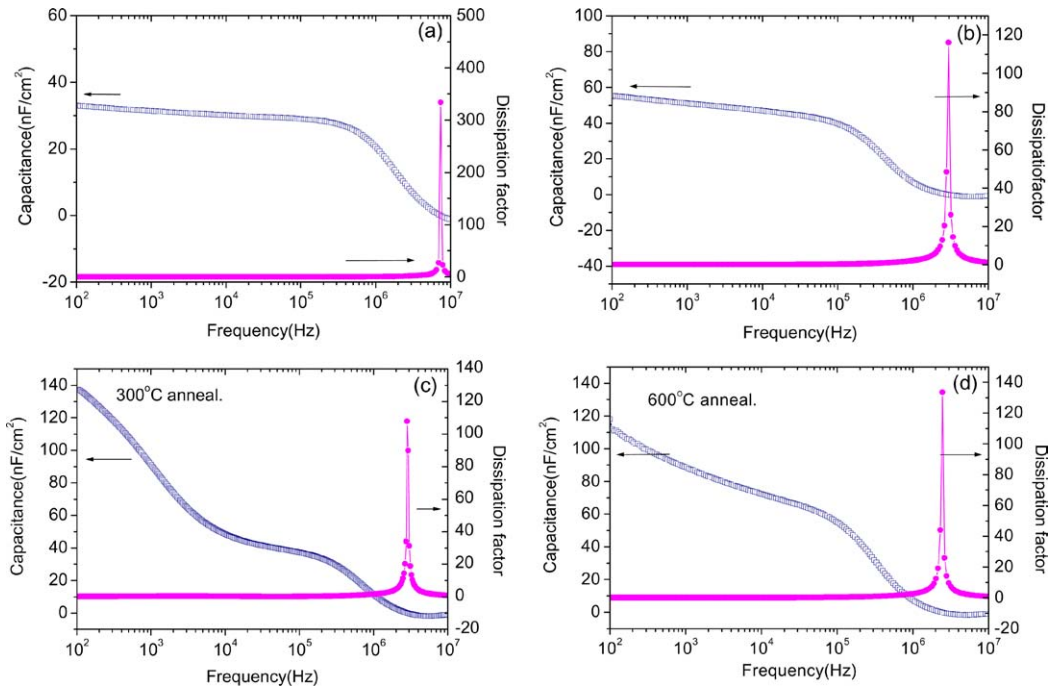


Fig. 5. Capacitance and dissipation factor of (a)  $\text{Al}_2\text{O}_3$ , (b)  $\text{Nb}_2\text{O}_5$  and  $\text{ZrO}_2$  annealed at (c)  $300^\circ\text{C}$  and (d)  $400^\circ\text{C}$ . The films were anodized up to 400 V.

various oxide films formed by anodizing up to 400 V. The capacitance and dissipation factor at 120 Hz of  $\text{Al}_2\text{O}_3$  layer (a) and  $\text{Nb}_2\text{O}_5/\text{Al-NbO}_x/\text{Al}_2\text{O}_3$  layer (b) are  $32.9 \text{ nF/cm}^2$ ,  $0.048$  and  $55.1 \text{ nF/cm}^2$ ,  $0.073$  respectively. The capacitance of  $\text{Nb}_2\text{O}_5/\text{Al-NbO}_x/\text{Al}_2\text{O}_3$  layer is higher 1.7 times compared to capacitance of  $\text{Al}_2\text{O}_3$  film. Figure 5(c) and (d) shows the dielectric properties of  $\text{ZrO}_2/\text{Al-ZrO}_x/\text{Al}_2\text{O}_3$  composite oxide anodized up to 400 V after annealing at 300 and  $600^\circ\text{C}$ , respectively. The capacitance and dissipation factor at 120 Hz are  $136 \text{ nF/cm}^2$ ,  $0.259$  and  $111 \text{ nF/cm}^2$ ,  $0.196$ , respectively. Although the thickness of  $\text{Al}_2\text{O}_3$  in films annealed at  $300^\circ\text{C}$  was thicker than that at  $600^\circ\text{C}$ , the capacitance of film at  $300^\circ\text{C}$  was higher. The dielectric properties of  $\text{ZrO}_2$  films without anodizing were surveyed in order to investigate this discrepancy. The capacitance and dissipation factor of only  $\text{ZrO}_2$  films annealed at 300 and  $600^\circ\text{C}$  show  $810 \text{ nF/cm}^2$ ,  $0.139$  and  $609 \text{ nF/cm}^2$ ,  $0.031$ , respectively. Therefore, the capacitance difference of composite oxide layer is due to the properties of  $\text{ZrO}_2$  film rather than that of  $\text{Al}_2\text{O}_3$ . The capacitance of  $\text{ZrO}_2/\text{Al-ZrO}_x/\text{Al}_2\text{O}_3$  anodized up to 400 V is 3 times larger than that of  $\text{Al}_2\text{O}_3$  film.

#### 4. Conclusion

$\text{ZrO}_2$  and  $\text{Nb}_2\text{O}_5$  films were coated on high purity aluminum foils by sol-gel method for application as dielectrics in aluminum electrolytic capacitor. Uniform  $\text{Nb}_2\text{O}_5$  and  $\text{ZrO}_2$  films were coated successfully on aluminum substrates. The  $\text{ZrO}_2$  films were crystallized even at  $300^\circ\text{C}$  and composed of nano-polycrystal. After the coated aluminum foils were anodized, the triple layer of  $\text{ZrO}_2(\text{Nb}_2\text{O}_5)/\text{Al-Zr}(\text{Nb})\text{O}_x/\text{Al}_2\text{O}_3$  was formed onto aluminum substrates. The  $\text{Al}_2\text{O}_3$  layer in  $\text{ZrO}_2$  film annealed at  $600^\circ\text{C}$  was thinner and denser than that without  $\text{ZrO}_2$  coating because a dense crystalline  $\text{ZrO}_2$  layer in surface inhibited the inward diffusion of  $\text{O}^{2-}$  ions from electrolyte. The  $\text{Al-Zr}(\text{Nb})\text{O}_x$  composite oxide layer was formed at interface between  $\text{ZrO}_2(\text{Nb}_2\text{O}_5)$  and Al substrate irrelevant to annealing temperature. The slopes of potential curve become flatter with increasing annealing temperature. The capacitance difference of composite oxide layer is due to the properties of  $\text{ZrO}_2$  film rather than that of  $\text{Al}_2\text{O}_3$ . The dielectric constant of  $\text{ZrO}_2$  and  $\text{Nb}_2\text{O}_5$  showed about 3 and 1.7 times compared to that of  $\text{Al}_2\text{O}_3$ , respectively.

**Acknowledgment**

This work was supported by grant No. (R05-2002-000-00862-0) from the Basic Research Program of the Korea Science & Engineering Foundation.

**References**

1. R.S. Alwitt, H. Uchi, T.R. Beck, and R.C. Alkire, *J. Electrochem. Soc.*, **131**, 13 (1997).
2. H. Takahashi, M. Nagatama, H. Akahori, and A. Kitahara, *J. Electron Microscopy*, **22**, 149 (1973).
3. H. Takahashi and M. Nagayama, *Electrochim. Acta*, **23**, 279 (1978).
4. M. Shikanai, M. Sakairi, H. Takahashi, M. Seo, K. Takahiro, and S. Yamaguchi, *J. Electrochem. Soc.*, **144**, 2756 (1997).
5. H. Takahashi, H. Kamada, M. Sakairi, K. Takahiro, S. Nagata, and S. Yamaguchi, 193rd Meeting Abstracts of the Electrochem. Soc., (1998) p. 207.
6. K. Watanabe, M. Sakairi, H. Takahashi, S. Hirai, and S. Yamaguchi, *J. Electroanal. Chem. Soc.*, **473**, 250 (1999).
7. K. Shimizu, G.E. Thompson, and G.C. Wood, *Thin Solid Films*, **81**, 39 (1981).
8. H. Takahashi and M. Nagayama, *Corros. Sci.*, **18**, 911 (1978).
9. Y. Xu, G.E. Thompson, G.C. Wood, and B. Bethune, *Corros. Sci.*, **27**, 83 (1987).
10. T. Kudo and R.S. Alwitt, *Electrochim. Acta*, **23**, 341 (1978).
11. K. Shimizu and K. Kobayashi, *J. Electrochem. Soc.*, **132**, 1384 (1985).
12. H. Takahashi, C Ikegami, M Seo, and R. Furuichi, *J. Electron Microsc.*, **40**, 101 (1991).
13. K. Watanabe, M. Sakairi, H. Takahashi, K. Takahiro, S. Nagata, and S. Hirai, *Electrochemistry*, **67**, 1243 (1999).